Source Apportionment Using Radiocarbon and Organic Tracers for $PM_{2.5}$ Carbonaceous Aerosols in Guangzhou, South China: Contrasting Local- and Regional-Scale Haze Events

Junwen Liu[1,4], Jun Li[1*], Yanlin Zhang[2], Di Liu[1], Ping Ding[3], Chengde Shen[3], Kaijun Shen[1,4], Quanfu He[1,4], Xiang Ding[1], Xinming Wang[1], Duohong Chen[1], Sönke Szidat[2], Gan Zhang[1]

[1]State Key Laboratory of Organic Geochemistry, Guangzhou Institute of Geochemistry, Chinese Academy of Sciences, Guangzhou, 510640, China
[2]Department of Chemistry and Biochemistry & Oeschger Centre for Climate Change Research, University of Bern, Berne, 3012, Switzerland
[3]State Key Laboratory of Isotope Geochemistry, Guangzhou Institute of Geochemistry, Chinese Academy of Sciences, Guangzhou, 510640, China
[4]University of Chinese Academy of Sciences, Beijing, 100049, China

[*]Corresponding author

Accepted version

Published in
Environmental Science and Technology 48 (2014) 12002-12011
http://dx.doi.org/10.1021/es503102w

Abstract

We conducted a source apportionment and investigated the atmospheric behavior of carbonaceous aerosols during hazy and normal days using radiocarbon (^{14}C) and biomass burning/secondary organic aerosol (SOA) tracers during winter in Guangzhou, China. Haze episodes were formed either abruptly by local emissions or through the accumulation of particles transported from other areas. The average contributions of fossil carbon to elemental carbon (EC), water-insoluble organic carbon, and water-soluble organic carbon were 71 ± 10%, 40 ± 6% and 33 ± 3%, respectively. High contributions of fossil carbon to EC (80−90%) were observed for haze samples that were substantially impacted by local emissions, as were the highest (lowest) ratios for NO_3^-/SO_4^{2-} (OC/EC), which indicates that these particles mainly came from local vehicle exhaust. Low contributions of fossil carbon to EC (60−70%) were found for haze particles impacted by regional transport. Secondary organic carbon (SOC) calculated using SOA tracers accounts for only ~20% of the SOC estimated by ^{14}C, which is probably because some important volatile organic carbons are not taken into account in the SOA tracer calculation method and because of the large discrepancy in ambient conditions between the atmosphere and smog chambers. A total of 33 ± 11% of the SOC was of fossil origin, a portion of which could be influenced by humidity.

Keywords: Haze, ^{14}C, organic tracer, secondary organic carbon, $PM_{2.5}$

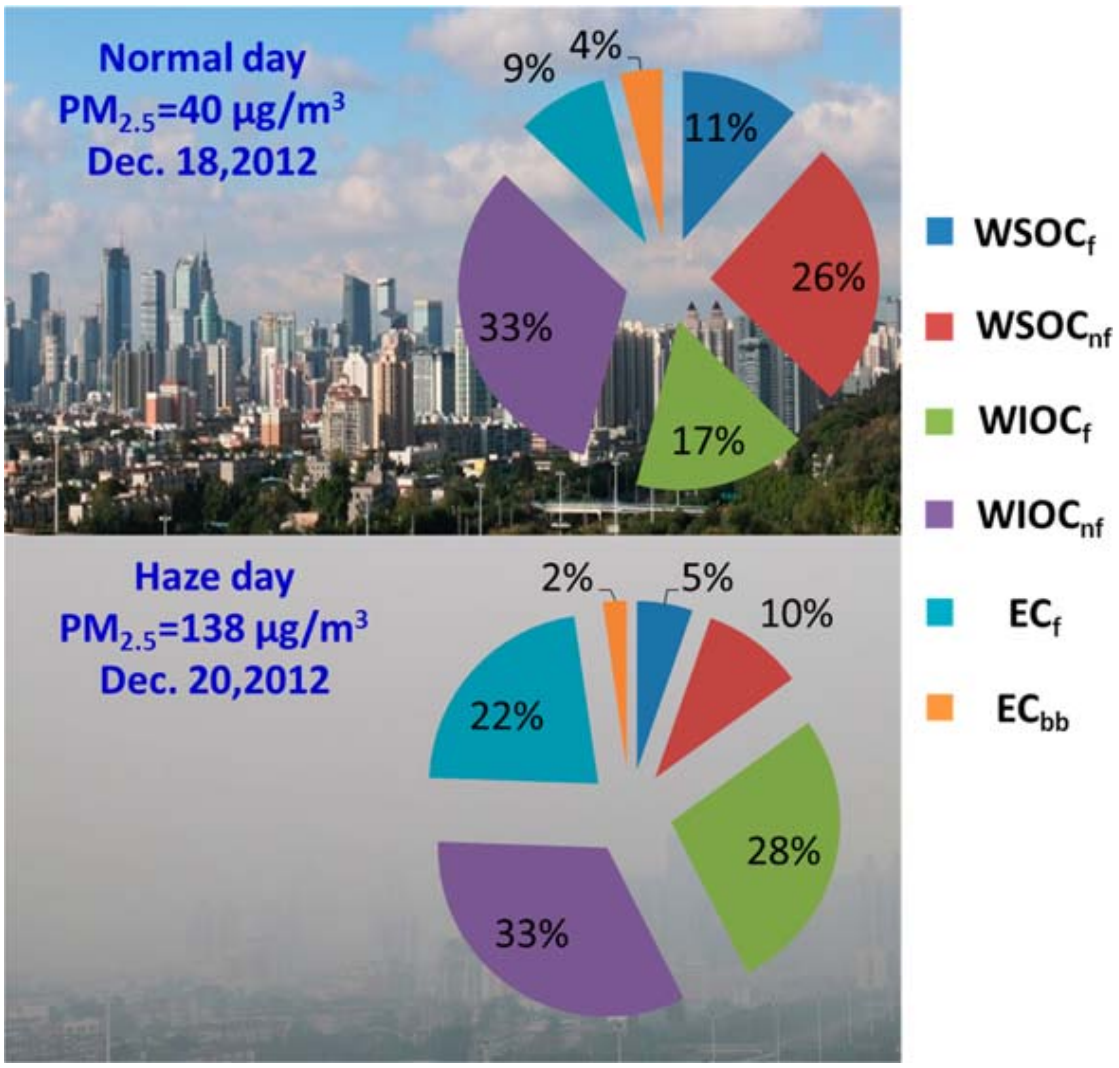
Normal day
PM2.5=40 μg/m3
Dec. 18,2012
9%
4%
11%
26%
33%
17%
Haze day
PM2.5=138 μg/m3
Dec. 20,2012
2%
5%
10%
22%
28%
33%
WSOCf
WSOCnf
WIOCf
WIOCnf
ECf
ECbb

TOC

1 Introduction

Haze episodes in China occur frequently, causing extensive public and scientific concern.[1,2] Haze particles exert a severe influence on not only human health and air quality,[2] but also the climatic system.[3] The main cause of this haze is the rapid or persistent enhancement of fine particle ($PM_{2.5}$, i.e., particles with an aerodynamic diameter less than 2.5 μm) concentrations in the air, accompanied by relatively stable synoptic conditions. These $PM_{2.5}$ particles can either be emitted from local sources or transported from other regions through atmospheric movement.

Carbonaceous aerosols account for a large fraction of $PM_{2.5}$ particles (~20−90%)[4] and are considered to be a vital constituent controlling the formation and evolution of haze episodes. Extremely high concentrations of carbonaceous aerosols (~100 μg C/m^3) have been recorded during typical haze days in northern China,[5] as well as in southern[6] and central China.[7] Generally, carbonaceous aerosols can be categorized into organic carbon (OC) and elemental carbon (EC) based on their thermal, chemical, and optical properties. EC is emitted directly from incomplete combustion (e.g., wood fire, traffic, and industry emissions) and is frequently used as a primary tracer due to its inert physiochemical properties in the atmosphere. OC includes primary sources of emission (e.g., biogenic sources, biomass burning, traffic, cooking, industry, soil, etc.) and secondary organic carbon (SOC), which is formed by the atmospheric oxidation of gaseous precursors.[4,8] Water-soluble organic

carbon (WSOC) mainly comprises compounds with polar functional groups, such as polyols, and (poly-)carboxylic acids;[9] these chemicals are mainly derived from primary biomass burning and SOC.[10,11] For episodes with limited biomass burning activity, WSOC is frequently used as an SOC tracer.[10,12] Water-insoluble organic carbon (WIOC) includes alkanes, polycyclic aromatic hydrocarbons, plant debris, and bacteria. Although carbonaceous aerosols play an important role in air pollution and haze formation, knowledge of their emission sources and atmospheric behavior (including the characteristics of biomass vs fossil fuel emissions and the differences between primary and secondary sources) are still poorly understood.

Radiocarbon (^{14}C) measurements allow unambiguous differentiation between fossil and nonfossil sources. The underlying principle of ^{14}C measurements is that this radioisotope has become extinct in fossil fuel carbon, while its contemporary level is relatively constant.[13,14] With a combination of organic tracers, detailed source apportionments of carbonaceous aerosols can be achieved via ^{14}C analysis. These data are very helpful to understand the evolution mechanisms of haze and SOC in the real atmosphere, with an aim of controlling pollutant emissions. So far, such studies are still scarce and have mainly been conducted in developed countries in Europe[15−18] or the United States.[19,20] Only a few studies have been performed in Chinese cities[21,22] or rural sites.[23,24]

Guangzhou (23.1°N, 113.3°E) is the largest city in the subtropical zone of

southern China, with a population of ~12 million. This city often suffers severe air pollution episodes: it has been reported that ~150 days per year may be governed by haze particles in Guangzhou.[6] Previous studies have shown that local haze particles are significantly affected by industrial and vehicular emissions,[25,26] while regional haze particles were strongly influenced by biomass burning.[26] However, unambiguous relative contributions of different emission sources cannot readily be estimated quantitatively. In this work, different carbon species (WIOC, WSOC, and EC) and water-soluble ions were measured, as well as three anhydrosugar isomers, i.e., levoglucosan (Lev), galactosan (Gal), and mannosan (Man), which are good markers of aerosols derived from biomass burning.[27,28] Eight samples representing different atmospheric conditions were selected to further analyze the ^{14}C content of WIOC, WSOC, and EC, as well as secondary organic aerosol (SOA) tracers that could directly reflect atmospheric reactions. To the best of our knowledge, the combination of SOA tracers, primary biomass burning tracers, and ^{14}C measurements in different carbonaceous fractions (EC, WSOC, and WIOC) has not yet been investigated in China. The objectives of this study are (1) to determine the chemical composition of $PM_{2.5}$; (2) to apportion a relative contribution of fossil fuel and contemporary carbon to carbonaceous aerosols using ^{14}C measurements and organic tracers; and (3) to provide an insight into the formation of haze particles and SOC.

2 Materials and methods

2.1 Sampling campaign

The sampling site is located at an urban site (Guangzhou Institute of Geochemistry, GIG) in Guangzhou, China (Figure 1), where no obvious point emission sources are found nearby. On the roof of the GIG library building (~20 m height), 48 daily 24-h $PM_{2.5}$ samples, as well as three field blank samples (exposed to air for 5 min), were collected on prebaked (450 °C, 6 h, muffle furnace) quartz fiber filters (QFF, 8 × 10 in., Pall) with a high-volume sampler (XT-1025, Shanghai XinTuo Analytical Instruments Co., Ltd.) at a flow of ~1 m^3/min from Nov. 29, 2012 to Jan. 19, 2013. After sampling, filters were folded, wrapped in aluminum foil, sealed in airtight plastic bags, and stored in a refrigerator at −20 °C until analysis.

2.2 Chemical analysis

To obtain the WSOC, EC, and WIOC fractions from a single punch filter, a circular section of the punch filter was clamped in place between a filter support and a funnel and then ultrapure water was slowly passed through the punch filter without a pump, allowing the WSOC to be extracted delicately. The remaining carbon on the filter was identified as WIOC or EC by an OC/EC analyzer (Sunset, U.S.) (Supporting Information, SI). WSOC was quantified as the total dissolved organic carbon in solution using a total organic carbon (TOC) analyzer (Shimadzu TOC_VCPH, Japan) following the nonpurgeable organic carbon protocol. We found that 100 mL of ultrapure water could remove ~100%

of WSOC, extracted by soaking for 12 h (SI Table S1). Thus, 100 mL of ultrapure water was used for experiments.

Methods associated with the analysis of water-soluble ions (Na^+, NH_4^+, K^+, Mg^{2+}, Ca^{2+}, SO_4^{2-}, NO_3^-, Cl^-),[29] anhydrosugars[23,30] and SOA tracers[31] have been described previously and are provided in the SI. The SOA tracers analyzed in this study include isoprene SOA tracers (cis-2-methyl-1,3,4-trihydroxy-1-butene, 3-methyl-2,3,4-trihydroxy-1-butene, trans-2-methyl-1,3,4-trihydroxy-1-butene, 2-methylglyceric acid, 2-methylthreitol, 2-methylerythritol), monoterpene SOA tracers (3-hydroxyglutaric acid, pinonic acid), a β-caryophyllene SOA tracer (β-carophyllene acid) and an aromatic SOA tracer (2,3-dihydroxy-4-oxopentanoic acid). These SOA tracers were converted into corresponding SOC concentrations by the carbon mass fraction of SOC (f_{soc}) as obtained by chamber experiments.[32]

2.3 Radiocarbon measurements

Isolation systems for WIOC and EC with regard to ^{14}C measurements at the Guangzhou Institute of Geochemistry have been described previously,[23,33] and details are provided in the SI. WSOC solution was frozen in a 40-mL glass vial and freeze-dried to dryness at −40 °C for 24 h using a freeze-dryer. A smaller quantity of water in solution favors the drying and transfer of WSOC in subsequent procedures; thus, 20 mL of ultrapure water, which could remove ~90% of WSOC (SI Table S1), was used to extract WSOC here. The WSOC residue was redissolved with ~500 μL of ultrapure water and then transferred

to a precombusted quartz tube, which was then placed in the freeze-dryer. After that, the quartz tube was combusted at 850°. Water extraction was performed at a clean bench (SW-CJ-1FD, Suzhou Purification Equipment Co., Ltd.). Finally, the corresponding evolved CO_2 (WIOC, EC, and WSOC) was cryo-trapped, quantified manometrically, sealed in a quartz tube and reduced to graphite at 600 °C using zinc with an iron (200 mg, Alfa Aesar, 1.5−3 mm, 99.99%) catalyst[34] for accelerator mass spectrometry (AMS) target preparation. Approximately 200 μg of carbon was prepared for each carbon fraction. The preparation of the graphite target was performed at the GIG, and the determination of the isotopic ratio was conducted at Peking University using a NEC compact AMS.

All ^{14}C results are expressed as the fraction of modern carbon (f_m) and have been corrected for $\delta^{13}C$ fractionation. f_m was further converted into the fraction of contemporary carbon (f_c) by normalization with a conversion factor of 1.10 and 1.06 for EC and OC, respectively, to compensate for the excess ^{14}C produced by nuclear bomb testing in the 1950 and 1960s.[24,35] Typically, uncertainties for the conversion factor are within 5%. Therefore, f_c can range from 0 (pure fossil fuel) to 1 (pure biogenic carbon) and directly reflects the relative biogenic contribution to carbon. It should be noted that the f_c values of OC (OC = WSOC + WIOC) and TC (TC = WSOC + WIOC + EC) here were calculated by isotopic mass balance. The carbon content of field blanks in this study was negligible (0.42 ± 0.08 μg/cm^2, less than 5% of the carbon content

measured in samples). Therefore, no field blank subtraction was performed for the ^{14}C measurements in this study.

3 Results and discussion

3.1 General remarks on $PM_{2.5}$ and chemical ratios

Concentrations of the various components in $PM_{2.5}$ collected in winter in Guangzhou are shown in Table 1. During the sampling campaign, $PM_{2.5}$ ranged from 38.7 to 138 μg/m^3 with an average of 74.6 ± 24.2 μg/m^3. A total of 100% and 40% of the measured $PM_{2.5}$ levels exceeded the First grade National Standard (35 μg/m^3, 24 h) and Second grade National Standard (75 μg/m^3, 24 h) of China, respectively. This implies that stricter regulations or laws associated with emissions are needed in Guangzhou to meet the national standard and to improve air quality efficiently. Generally, $PM_{2.5}$ concentrations correlated negatively with wind strength and precipitation (Figure 2), with the highest values appearing when wind speeds were lowest (Dec. 13−14, Dec. 20−21, Dec. 25−26, and Jan. 14−15) and the lowest values generally appearing with the strongest winds and highest precipitation (Dec. 01−02, Dec. 18−19, Jan. 04−05). This suggests that both the scavenging effect of rain and dilution effect of wind have clear positive elimination influences on $PM_{2.5}$ concentrations, as well as indirectly reflecting the high intensity of local $PM_{2.5}$ emissions in Guangzhou.

The dominant species are SO_4^{2-} (10.6±4.4 μg/m^3), WIOC (6.7±4.0 μg/m3), NO_3^- (5.8±3.5 μg/m^3), NH_4^+ (5.1±2.1 μg/m^3), WSOC (4.1±2.0 μg/m^3), and EC

(2.1±1.7 μg/m^3) (Table 1), accounted for 14.3±4.6%, 8.6±3.2%, 7.3±2.7%, 6.7±1.5%, 5.3±1.7% and 2.6±1.4% to $PM_{2.5}$, respectively. Obvious variations of chemical compositions are observed with the change of $PM_{2.5}$ and meteorological parameters (Figure 2), indicating the various sources of $PM_{2.5}$ in Guangzhou and complicated atmospheric behaviors of chemical species. High peaks of NO_3^-/SO_4^{2-} generally correlated with low peaks of OC/EC (Dec. 09-10, Dec. 16-17, Dec. 20-22, Dec. 24-25, Jan. 01-02 and Jan. 15-16), indicating important influence from traffic exhausts on these samples, because high NO_3^-/SO_4^{2-} [36] and low OC/EC[16] are characteristic for PM freshly produced by vehicles. Since particles directly come from biomass burning show a characteristic of both high values of OC/EC and Lev/OC[16], impact of biomass burning is suspected on the samples collected during Dec. 26-27, Dec. 11-12 and Jan. 17-18). A process of $PM_{2.5}$ accumulation is observed during Jan. 04 to Jan. 12 when wind speeds are moderate and stable, of which synoptic conditions apparently beneficial to the accumulation of particles derived either from local or regional sources. OC/EC ratios also show an increasing trend during this period, which is likely due to the input of biomass burning aerosols evidenced by higher Lev/OC. However, OC/EC rises to the highest ratio even when Lev/OC declines visibly (Jan. 09-12) during this period, which we attribute to the OC enrichment during SOC formation. This example suggests that the haze formation in Guangzhou is highly complicated and may be triggered by multiple sources and atmospheric processes. Other episodes with high $PM_{2.5}$

level (>100 μg/m^3) show a similar behavior.

3.2 ^{14}C results: fraction of modern carbon (f_m)

To further investigate the sources of fine carbonaceous particles and haze formation, eight samples representing different $PM_{2.5}$ loadings, chemical compositions and meteorological conditions were selected to be analyzed for ^{14}C signals (Figure 2). Sample GIG01 and GIG03 with the highest wind speeds and the lowest $PM_{2.5}$ concentrations represent the regional background samples. Sample GIG02 with the lowest wind speed and the highest $PM_{2.5}$ concentration represents a typical haze of quick accumulation. Samples GIG04−GIG08 showed a process of $PM_{2.5}$ gradual accumulation when wind speeds were moderate and stable. Of which samples GIG02, GIG06, GIG07, and GIG08 were collected during typical haze episodes with $PM_{2.5}$ concentrations >100 μg/m^3.

The average f_m values for WSOC, WIOC, and EC were 0.71 ± 0.03, 0.64 ± 0.06, and 0.31 ± 0.11, respectively, suggesting that fossil fuel has the largest impact on EC, whereas WIOC and WSOC are affected more by nonfossil sources. The trend of f_m(WSOC) > f_m(WIOC) > f_m(EC) has also been observed in other urban regions, such as Göteborg and Zürich.[15,37]

Because EC is formed only by primary emission, is inert in ambient air and originates from wood burning or fossil fuel combustion only, f_m(EC) particularly tracks the change of these $PM_{2.5}$ sources. Its high relative standard deviation of 35% shows a large variability of wood burning and fossil impacts. Two

different trends of fm(EC) are observed in $PM_{2.5}$ concentrations (Figure 3). On one hand, GIG02 and GIG08 have the lowest f_m(EC) values. Compared to the other samples, these two haze samples were impacted by fossil emissions from local sources (especially traffic exhaust) based on their much higher NO_3^-/SO_4^{2-} ratios (~1), lowest OC/EC ratios and substantially lowest winds (~1 m/s) (Figure 2), which suggests that atmospheric transport is limited for particles from outside Guangzhou. This also implies that particles emitted by local sources in Guangzhou are depleted of biomass-burning EC, which is supported by the low Lev/OC values for GIG02 and GIG08. On the other hand, the two haze samples GIG06 and GIG07 show a higher f_m(EC) level (~0.35), which is similar to that observed in normal samples with the lowest PM2.5 levels. Unlike GIG02 and GIG08, samples GIG06 and GIG07 were collected step by step through an accumulation process from Jan. 04 to Jan. 12 (Figure 2), experiencing a significant impact from biomass-burning particles based on the higher Lev/OC ratios. According to their wind speed, these aerosols were transported from outside of Guangzhou.

The variability of f_m(WIOC) and f_m(WSOC) is much smaller than that of f_m(EC), with relative standard deviations of ~9% and ~4%, respectively. Still, the f_m(WIOC) and f_m(WSOC) values for GIG08 and GIG02 are slightly lower than those for GIG06 and GIG07, which may be explained as follows. TC emitted by biomass burning is significantly enriched with OC (~80%),[16] while the OC content is reduced to ~30% (consisting mainly of WIOC) in traffic exhaust,[38]

which contributes to the fact that OC is dominantly controlled by contemporary carbon in both rural[24] and urban areas.[13,15] We thus assume that the fossil OC emitted in Guangzhou is not sufficient to cause a detectable change in f_m(WIOC) and f_m(WSOC). In addition, ambient temperature and humidity may also have an influence on f_m(WIOC) and f_m(WSOC) due to the formation of SOC, which we will discuss in the following sections.

3.3 Source apportionment based on ^{14}C

On the basis of f_c values (Table 2), the carbon fractions can be divided into fossil (f) and nonfossil (nf) sources. Because EC is derived from only biomass burning (bb) and fossil fuel combustion, the fraction of nonfossil fuel EC is expressed as EC_{bb} here. Figure 4 displays the relative contributions of fossil and nonfossil sources to the EC, WSOC, and WIOC fractions in winter in Guangzhou. On average, $WIOC_{nf}$ is the largest contributor to the TC, accounting for 29 ± 3%, followed by $WIOC_f$ (22 ± 6%), $WSOC_{nf}$ (22 ± 7%), $WSOC_f$ (11 ± 4%), EC_f (14 ± 6%), and EC_{bb} (3 ± 1%). The contribution of fossil fuel sources to WIOC (40 ± 6%) is slightly lower than that of nonfossil sources (60 ± 6%). This is comparable to previous studies conducted in European urban cities such as Göteborg (55 ± 8%)[15] and Zürich (70 ± 7%).[37] Most of the WSOC (67 ± 3%) is derived from nonfossil fuel emission sources in this study, which is reasonable because OC directly emitted from the combustion of fossil fuel is mainly water insoluble.[10] However, these values are lower than those observed in European and American cities (~70−85%);[10,15,37] this variation is likely because more

SOC is derived from fossil fuels in Guangzhou, given that WSOC is a good tracer for SOC in urban regions.[11,39] As expected, in Guangzhou, EC is largely dominated by the combustion of fossil fuel (71 ± 10%), which is comparable to other studies performed in cities around the world, such as Beijing (83 ± 4%),[22] Göteborg (89 ± 3%),[15] Zürich (75 ± 5%),[40] and represents a value much higher than found in samples collected at rural stations (25−50%) in southern China[24] and southern Asia (45−52%).[41]

The EC_f content of GIG02 (22%) and GIG08 (17%) is ~2−4 times higher than in other samples (5−10%), which can be attributed to the significance of local sources for GIG02 and GIG08. On the contrary, no significant differences between the samples are observed for EC_{bb} (2−4%). Due to the substantial invasion of biomass-burning particles from Jan. 04 to Jan. 12, the relative contribution of $WIOC_f$ declined gradually from 27% (GIG04) and 20% (GIG05) to 13% (GIG06 and GIG07), and the $WSOC_f$ and $WSOC_{nf}$ content increased; these changes indicate that more SOC had been formed. Similar carbon compositions are observed for GIG01 and GIG03, most likely because these two samples come from more remote regions characterized by both the lowest NO_3^-/SO_4^{2-} [42] and Lev/OC (Figure 2). Remote particles generally have a high proportion of SOC[43] due to the longer-range atmospheric transport they experience (Figure 1).

3.4 Tracer-based biomass-burning OC

^{14}C alone cannot discriminate among sources of contemporary carbon

(biomass burning, biological emissions and biogenic SOC). Biomass burning OC (OC_{bb}) is frequently calculated as the ratio $(OC/Lev)_{bb}$ in fresh biomass burning aerosols on the basis that Lev is an prominent tracer for biomass burning tracer to its high concentration and stable physiochemical properties in the atmosphere.[27]

$OC_{bb} = Lev \times (OC/Lev)_{bb}$

The remaining contemporary OC (OC_{bio}) content can be calculated by the following equation:

$OC_{bio} = OC_{nf} – OC_{bb}$

OC_{bio} includes primary biological aerosols (OC_{bio_pri}) (pollen, spore, plant debris, etc.) and biogenic SOC (OC_{bio_sec}). $(OC/Lev)_{bb}$ ratios vary with different biomass types (hardwood, softwood, and annual plants, such as grass) (SI Table S2) due to differences in cellulose content. On the basis of the ratios of the three anhydrosugar isomers,[28] biomass-burning aerosols in Guangzhou mainly originate from hardwood combustion (SI Table S2). Therefore, an $(OC/Lev)_{bb}$ ratio of 7.76 ± 1.47 (SI Table S2) was used to calculate OC_{bb} in this study. As expected, GIG04, GIG05, GIG06, and GIG07 had the highest OC_{bb} content relative to OC (30−50%), as these samples were obviously impacted by biomass burning. Lower proportions were found for samples influenced by local sources (GIG02 and GIG08, 20−30%) and samples from remote areas (GIG01 and GIG03, <20%).

3.5 Contributions of fossil fuel and biogenic carbon to SOC

One of the scientific issues associated with SOC in the urban atmosphere is the relative contributions of fossil and nonfossil precursors, which has been discussed intensively for a long time. However, there is still no method available to measure the SOC derived directly from these two sources. The combination of f_m(OC) analysis with aerodyne aerosol mass spectrometer measurements has previously allowed the sources of semivolatile oxygenated organic carbon (SV−OOC) to be quantified as 71% fossil and 29% nonfossil in Los Angeles.[20] Recently, Zhang et al. reported that $WSOC_f$ can serve as a good proxy of fossil fuel SOC ($OCf_{\_sec}$),[24] based on previous observations that OC freshly emitted from the combustion of fossil fuel is mostly water insoluble.[10,44,45] In this study, $WSOC_f$ is significantly correlated with 2,3-dihydroxy-4-oxopentanoic acid ($r = 0.95$, $p < 0.01$, SI Figure S1), which further validates the understanding that $WSOC_f$ originates from the atmospheric oxidation of fossil VOCs. No significant correlation ($r = 0.42$, $p = 0.31$) was found between $WSOC_f$ and EC_f (SI Figure S2), which demonstrates that $WSOC_f$ is formed by atmospheric reaction rather than direct emission. Thus, $WSOC_f$ can reasonably be regarded as OC_{f_sec}.

Compared with OC_{f_sec}, the estimation of OC_{bio_sec} is more complicated due to the inclusion of OC_{bio_pri} in OC_{bio}. Here, OC_{bio} is significantly correlated with most biogenic SOA tracers at confidence levels of 95% and 99% (SI Figure S1), which indicates that OC_{bio} likely consists largely of OC_{bio_sec}. OC_{bio} also correlated well with temperature ($r = 0.93$, $p < 0.01$), providing further evidence for the dominance of OC_{bio_sec} within OC_{bio}, as SOC formation is more favorable

at higher temperature. In addition, according to previous studies based on direct measurements of OC_{bio_pri}, the proportion of OC_{bio_pri} generally accounted for only ~1−5% of OC in fine particles in Europe[16] and ~1% in China.[46] Thus, OC_{bio_pri} has frequently been neglected when calculating SOC concentrations;[44,47] this approach is adopted here as well. Table 3 shows the respective SOC concentrations calculated from ^{14}C values and SOA tracers. On average, $SOC_{M+I+\beta}$ and SOC_A explain 19 ± 8% of OC_{bio_sec} and 19 ± 7% of OC_{f_sec}, respectively. Because SOC values derived from SOA tracers ($SOC_{M+I+\beta}$ plus SOC_A) accounted for only 14 ± 6% of the OC in this study and because this proportion seems to be much lower than that observed in previous studies conducted in winter in southern and northern China (30−60%),[48,49] we assumed that the SOC values based on these SOA tracers is underestimated. A similar low value (~10%, on average) based on the SOA tracer method was reported in another study in fall and winter in Guangzhou.[31] Several factors could explain this result. First, the large discrepancy between ambient conditions in the real atmosphere and in chamber experiments may lead to large uncertainties for the f_{soc} values of SOA tracers. Second, some important fossil aromatic VOCs are missing. In the chamber experiment, only toluene was taken into account as an aromatic VOC. However, toluene accounted for only ~20% of the total aromatic VOCs emitted from vehicles during a tunnel study conducted in a southern Chinese city.[50] Other chemicals such as benzene, ethylbenzene, and m,p-xylene could contribute approximately 50% to SOC formation.[51] This is

consistent with the results noted earlier, in which 19 ± 7% of OC_{f_sec} was identified as SOC_A. Third, VOCs emitted from biomass burning might not be negligible. It has been reported that ~50% and ~15% of VOCs[52] were derived from biomass burning at regional and suburban sites in Guangzhou, respectively. Approximately 60−80% of the VOCs emitted by biomass burning are alkanes and alkenes,[50] whose contribution to SOC can approach ~20%.[51,53] Therefore, neglecting VOCs derived from biomass burning would also underestimate the contemporary SOC fraction, especially in winter when biomass burning is the most severe.

In this study, 46 ± 15% of OC could be explained by SOC (OC_{bio_sec} plus OC_{f_sec}), which is comparable to results obtained in other studies performed in Guangzhou during the winter season (36−42%).[49] As mentioned above, due to longer transport times, GIG01 and GIG03 have the largest SOC content relative to OC, ~60% and ~66%, respectively. The relative contribution of OC_{f_sec} to total SOC is 33 ± 11%, and the corresponding value for OC_{bio_sec} is 67 ± 11%, demonstrating that VOCs derived from biogenic/biomass burning emissions are the dominant contributor to SOC in Guangzhou, despite the importance of fossil emissions. The OC_{bio_sec} contribution calculated here is lower than the previous global inventory (~90%),[4] while comparable to recent estimates conducted in other polluted cities, such as Mexico City (~70%)[53] and Beijing (~50%).[46]

Because fossil-derived VOCs are less polar and appear to be more hydrophobic than biogenic VOCs, competing effects may exist between the

formation of OC_{f_sec} and OC_{bio_sec} due to changes in relative humidity.[44] Therefore, lower relative humidity should favor the formation of OC_{f_sec} over OC_{bio_sec}. In this study, humidity has a negative impact on OC_{f_sec}/SOC (except for GIG03 and GIG04) (Figure 5), which supports the above hypothesis. Obviously, the OC_{f_sec}/SOC ratio for GIG04 is much higher than expected. This is because the temperature of GIG04 was the lowest (5.8 °C) during sampling (Figure 2), which limits the emission of biogenic VOCs, while emissions should be independent of temperature for fossil-derived VOCs. Although the temperature of GIG03 was also very low, its OC_{f_sec}/SOC ratio is lower than expected. Given that this sample was collected when the wind speed was the highest and had the longest atmospheric transport time (Figure 1), we assume that a large fraction of the SOC from GIG03 may have been formed during transport, and the local humidity may play a limited role in the competing effects of formation for OC_{f_sec} and OC_{bio_sec}.

Acknowledgements

This work was supported by the “Strategic Priority Research Program (B)” of the Chinese Academy of Sciences (Grant No. XDB05040503), the Natural Science Foundation of China (NSFC; No.41125014 and 41273117), the Fund of the State Key Laboratory of Organic Geochemistry (No. SKLOG2013A01) and the Guangzhou Elites Scholarship Council (JY201332).

References

(1) He, H.; Wang, Y.; Ma, Q.; Ma, J.; Chu, B.; Ji, D.; Tang, G.; Liu, C.; Zhang,

H.; Hao, J. Mineral dust and NOx promote the conversion of SO2 to sulfate in heavy pollution days. Sci. Rep. 2014, 4, 4172.

(2) Liu, X. G.; Li, J.; Qu, Y.; Han, T.; Hou, L.; Gu, J.; Chen, C.; Yang, Y.; Liu, X.; Yang, T.; Zhang, Y.; Tian, H.; Hu, M. Formation and evolution mechanism of regional haze: a case study in the megacity Beijing, China. Atmos. Chem. Phys. 2013, 13 (9), 4501−4514.

(3) Wang, Y.; Wang, M.; Zhang, R.; Ghan, S. J.; Lin, Y.; Hu, J.; Pan, B.; Levy, M.; Jiang, J. H.; Molina, M. J. Assessing the effects of anthropogenic aerosols on Pacific storm track using a multiscale global climate model. Proc. Natl. Acad. Sci. U. S. A. 2014, 111, 6894−6899.

(4) Kanakidou, M.; Seinfeld, J. H.; Pandis, S. N.; Barnes, I.; Dentener, F. J.; Facchini, M. C.; Van Dingenen, R.; Ervens, B.; Nenes, A.; Nielsen, C. J.; Swietlicki, E.; Putaud, J. P.; Balkanski, Y.; Fuzzi, S.; Horth, J.; Moortgat, G. K.; Winterhalter, R.; Myhre, C. E. L.; Tsigaridis, K.; Vignati, E.; Stephanou, E. G.; Wilson, J. Organic aerosol and global climate modelling: a review. Atmos. Chem. Phys. 2005, 5 (4), 1053−1123.

(5) Zhao, X.; Zhao, P.; Xu, J.; Meng, W.; Pu, W.; Dong, F.; He, D.; Shi, Q. Analysis of a winter regional haze event and its formation mechanism in the North China Plain. Atmos. Chem. Phys. 2013, 13 (11), 5685−5696.

(6) Deng, X.; Tie, X.; Wu, D.; Zhou, X.; Bi, X.; Tan, H.; Li, F.; Jiang, C. Long-term trend of visibility and its characterizations in the Pearl River Delta (PRD) region, China. Atmos. Environ. 2008, 42 (7), 1424−1435.

(7) Zhang, F.; Cheng, H.-R.; Wang, Z.-W.; Lv, X.-P.; Zhu, Z.-M.; Zhang, G.; Wang, X.-M. Fine particles (PM2.5) at a CAWNET background site in Central China: Chemical compositions, seasonal variations and regional pollution events. Atmos. Environ. 2014, 86 (0), 193−202.

(8) Pöschl, U. Atmospheric aerosols: Composition, transformation, climate and health effects. Angew. Chem., Int. Ed. 2005, 44 (46), 7520−7540.

(9) Sullivan, A. P.; Weber, R. J. Chemical characterization of the ambient organic aerosol soluble in water:1. Isolation of hydrophobic and hydrophilic fractions with a XAD-8 resin. J. Geophys. Res.: Atmos. 2006, 111 (D5), D05314.

(10) Weber, R. J.; Sullivan, A. P.; Peltier, R. E.; Russell, A.; Yan, B.; Zheng, M.; De Gouw, J.; Warneke, C.; Brock, C.; Holloway, J. S. A study of secondary organic aerosol formation in the anthropogenic influenced southeastern United States. J. Geophys. Res.: Atmos. 2007, 112 (D13), D13302.

(11) Ding, X.; Zheng, M.; Yu, L.; Zhang, X.; Weber, R. J.; Yan, B.; Russell, A. G.; Edgerton, E. S.; Wang, X. Spatial and seasonal trends in biogenic secondary organic aerosol tracers and water-soluble organic carbon in the southeastern United States. Environ. Sci. Technol. 2008, 42 (14), 5171−5176.

(12) Docherty, K. S.; Stone, E. A.; Ulbrich, I. M.; DeCarlo, P. F.; Snyder, D. C.; Schauer, J. J.; Peltier, R. E.; Weber, R. J.; Murphy, S. M.; Seinfeld, J. H. Apportionment of primary and secondary organic aerosols in Southern California during the 2005 Study of Organic Aerosols in Riverside (SOAR-1). Environ. Sci. Technol. 2008, 42 (20),7655−7662.

(13) Szidat, S.; Jenk, T. M.; Gäggeler, H. W.; Synal, H. A.; Fisseha, R.; Baltensperger, U.; Kalberer, M.; Samburova, V.; Reimann, S.; Kasper-Giebl, A.; Hajdas, I. Radiocarbon (14C)-deduced biogenic and anthropogenic contributions to organic carbon (OC) of urban aerosols from Zürich, Switzerland. Atmos. Environ. 2004, 38 (24), 4035−4044.

(14) Szidat, S. Sources of Asian Haze. Science 2009, 323 (5913), 470−471.

(15) Szidat, S.; Ruff, M.; Perron, N.; Wacker, L.; Synal, H.-A.; Hallquist, M.; Shannigrahi, A. S.; Yttri, K.; Dye, C.; Simpson, D. Fossil and non-fossil sources of organic carbon (OC) and elemental carbon (EC) in Göteborg, Sweden. Atmos. Chem. Phys. 2009, 9 (5), 1521−1535.

(16) Gelencsér, A.; May, B.; Simpson, D.; Sánchez-Ochoa, A.; Kasper-Giebl, A.; Puxbaum, H.; Caseiro, A.; Pio, C.; Legrand, M. Source apportionment of PM2.5 organic aerosol over Europe: Primary/secondary, natural/anthropogenic, and fossil/biogenic origin. J. Geophys. Res.: Atmos. 2007, 112 (D23), D23S04.

(17) Yttri, K.; Simpson, D.; Stenström, K.; Puxbaum, H.; Svendby, T. Source apportionment of the carbonaceous aerosol in Norway − quantitative estimates based on 14C, thermal-optical and organic tracer analysis. Atmos. Chem. Phys. 2011, 11 (17), 9375−9394.

(18) Zotter, P.; Ciobanu, V. G.; Zhang, Y. L.; El-Haddad, I.; Macchia, M.; Daellenbach, K. R.; Salazar, G. A.; Huang, R. J.; Wacker, L.; Hueglin, C.; Piazzalunga, A.; Fermo, P.; Schwikowski, M.; Baltensperger, U.; Szidat, S.; Prévôt, A. S. H. Radiocarbon analysis of elemental and organic carbon in

Switzerland during winter-smog episodes from 2008 to 2012-Part I: Source apportionment and spatial variability. Atmos. Chem. Phys. Discuss. 2014, 14, 15591−15643.

(19) Schichtel, B. A.; Malm, W. C.; Bench, G.; Fallon, S.; McDade, C. E.; Chow, J. C.; Watson, J. G., Fossil and contemporary fine particulate carbon fractions at 12 rural and urban sites in the United States. J. Geophys. Res.: Atmos. 2008, 113, (D02311).

(20) Zotter, P.; El-Haddad, I.; Zhang, Y.; Hayes, P. L.; Zhang, X.; Lin, Y.-H.; Wacker, L.; Schnelle-Kreis, J.; Abbaszade, G.; Zimmermann, R. Diurnal cycle of fossil and nonfossil carbon using radiocarbon analyses during CalNex. J. Geophys. Res.: Atmos. 2014, 119, 6818−6835.

(21) Yang, F.; He, K.; Ye, B.; Chen, X.; Cha, L.; Cadle, S.; Chan, T.; Mulawa, P. One-year record of organic and elemental carbon in fine particles in downtown Beijing and Shanghai. Atmos. Chem. Phys. 2005, 5 (6), 1449−1457.

(22) Chen, B.; Andersson, A.; Lee, M.; Kirillova, E. N.; Xiao, Q.; Kruså, M.; Shi, M.; Hu, K.; Lu, Z.; Streets, D. G. Source forensics of black carbon aerosols from China. Environ. Sci. Technol. 2013, 47 (16), 9102−9108.

(23) Liu, D.; Li, J.; Zhang, Y.; Xu, Y.; Liu, X.; Ding, P.; Shen, C.; Chen, Y.; Tian, C.; Zhang, G. The use of levoglucosan and radiocarbon for source apportionment of PM2.5 carbonaceous aerosols at a background site in East China. Environ. Sci. Technol. 2013, 47 (18), 10454−10461.

(24) Zhang, Y.; Li, J.; Zhang, G.; Zotter, P.; Huang, R.-J.; Tang, J.; Wacker, L.;

Prévôt, A.; Szidat, S. Radiocarbon-based source apportionment of carbonaceous aerosols at a regional background site on Hainan Island, South China. Environ. Sci. Technol. 2014, 48, 2651−2659.

(25) Tan, J.; Guo, S.; Ma, Y.; Duan, J.; Cheng, Y.; He, K.; Yang, F. Characteristics of particulate PAHs during a typical haze episode in Guangzhou, China. Atmos. Res. 2011, 102 (1−2), 91−98.

(26) Andreae, M. O.; Schmid, O.; Yang, H.; Chand, D.; Yu, J. Z.; Zeng, L. M.; Zhang, Y. H. Optical properties and chemical composition of the atmospheric aerosol in urban Guangzhou, China. Atmos. Environ. 2008, 42 (25), 6335−6350.

(27) Simoneit, B. R. T.; Schauer, J. J.; Nolte, C. G.; Oros, D. R.; Elias, V. O.; Fraser, M. P.; Rogge, W. F.; Cass, G. R. Levoglucosan, a tracer for cellulose in biomass burning and atmospheric particles. Atmos. Environ. 1999, 33 (2), 173−182.

(28) Sang, X. F.; Gensch, I.; Laumer, W.; Kammer, B.; Chan, C. Y.; Engling, G.; Wahner, A.; Wissel, H.; Kiendler-Scharr, A. Stable carbon isotope ratio analysis of anhydrosugars in biomass burning aerosol particles from source samples. Environ. Sci. Technol. 2012, 46 (6), 3312−3318.

(29) Wang, X.; Ding, X.; Fu, X.; He, Q.; Wang, S.; Bernard, F.; Zhao, X.; Wu, D. Aerosol scattering coefficients and major chemical compositions of fine particles observed at a rural site in the central Pearl River Delta, South China. J. Environ. Sci. 2012, 24 (1), 72−77.

(30) Liu, J.; Xu, Y.; Li, J.; Liu, D.; Tian, C.; Chaemfa, C.; Zhang, G. The

distribution and origin of PAHs over the Asian marginal seas, the Indian and the Pacific Oceans: implications for outflows from Asia and Africa. J. Geophys. Res.: Atmos. 2014, 119, 1949−1961.

(31) Ding, X.; Wang, X. M.; Gao, B.; Fu, X. X.; He, Q. F.; Zhao, X. Y.; Yu, J. Z.; Zheng, M. Tracer-based estimation of secondary organic carbon in the Pearl River Delta, south China. J. Geophys. Res.: Atmos. 2012, 117 (D5), D05313.

(32) Kleindienst, T. E.; Jaoui, M.; Lewandowski, M.; Offenberg, J. H.; Lewis, C. W.; Bhave, P. V.; Edney, E. O. Estimates of the contributions of biogenic and anthropogenic hydrocarbons to secondary organic aerosol at a southeastern US location. Atmos. Environ. 2007, 41 (37), 8288−8300.

(33) Zhang, Y. L.; Liu, D.; Shen, C. D.; Ding, P.; Zhang, G. Development of a preparation system for the radiocarbon analysis of organic carbon in carbonaceous aerosols in China. Nucl. Instrum. Methods Phys. Res. Sect. B 2010, 268 (17−18), 2831−2834.

(34) Xu, X.; Trumbore, S. E.; Zheng, S.; Southon, J. R.; McDuffee, K. E.; Luttgen, M.; Liu, J. C. Modifying a sealed tube zinc reduction method for preparation of AMS graphite targets: Reducing background and attaining high precision. Nucl. Instrum. Methods Phys. Res. Sect. B 2007, 259 (1), 320−329.

(35) Mohn, J.; Szidat, S.; Fellner, J.; Rechberger, H.; Quartier, R.; Buchmann, B.; Emmenegger, L. Determination of biogenic and fossil CO2 emitted by waste incineration based on 14CO2 and mass balances. Bioresour. Technol. 2008, 99 (14), 6471−6479.

(36) Wang, Y.; Zhuang, G.; Tang, A.; Yuan, H.; Sun, Y.; Chen, S.; Zheng, A. The ion chemistry and the source of PM2.5 aerosol in Beijing. Atmos. Environ. 2005, 39 (21), 3771−3784.

(37) Zhang, Y.; Perron, N.; Prévôt, A.; Wacker, L.; Szidat, S. Fossil and non-fossil sources of different carbonaceous fractions in fine and coarse particles by radiocarbon measurement. Radiocarbon 2013, 55 (2), 1510−1520.

(38) He, L.-Y.; Hu, M.; Zhang, Y.-H.; Huang, X.-F.; Yao, T.-T. Fine particle emissions from on-road vehicles in the Zhujiang Tunnel, China. Environ. Sci. Technol. 2008, 42 (12), 4461−4466.

(39) Miyazaki, Y.; Kondo, Y.; Takegawa, N.; Komazaki, Y.; Fukuda, M.; Kawamura, K.; Mochida, M.; Okuzawa, K.; Weber, R., Timeresolved measurements of water-soluble organic carbon in Tokyo. J. Geophys. Res.: Atmos. 2006, 111, (D23).

(40) Szidat, S.; Jenk, T. M.; Synal, H.-A.; Kalberer, M.; Wacker, L.; Hajdas, I.; Kasper-Giebl, A.; Baltensperger, U. Contributions of fossil fuel, biomass-burning, and biogenic emissions to carbonaceous aerosols in Zurich as traced by 14C. J. Geophys. Res.: Atmos. 2006, 111 (D7), D07206.

(41) Gustafsson, Ö.; Kruså, M.; Zencak, Z.; Sheesley, R. J.; Granat, L.; Engström, E.; Praveen, P. S.; Rao, P. S. P.; Leck, C.; Rodhe, H. Brown clouds over south Asia: Biomass or fossil fuel combustion? Science 2009, 323 (5913), 495−498.

(42) Zhang, X.; Wang, Y.; Niu, T.; Zhang, X.; Gong, S.; Zhang, Y.; Sun, J.

Atmospheric aerosol compositions in China: spatial/temporal variability, chemical signature, regional haze distribution and comparisons with global aerosols. Atmos. Chem. Phys. 2012, 12 (2), 779−799.

(43) Ho, K.; Lee, S.; Cao, J.; Li, Y.; Chow, J. C.; Watson, J. G.; Fung, K. Variability of organic and elemental carbon, water soluble organic carbon, and isotopes in Hong Kong. Atmos. Chem. Phys. 2006, 6 (12), 4569−4576.

(44) Favez, O.; Sciare, J.; Cachier, H.; Alfaro, S. C.; Abdelwahab, M. M. Significant formation of water-insoluble secondary organic aerosols in semi-arid urban environment. Geophys. Res. Lett. 2008, 35 (15), L15801.

(45) Park, S. S.; Jeong, J.-U.; Cho, S. Y. Group separation of watersoluble organic carbon fractions in ash samples from a coal combustion boiler. As. J. Atmos. Environ. 2012, 6 (1), 67−72.

(46) Guo, S.; Hu, M.; Guo, Q.; Zhang, X.; Zheng, M.; Zheng, J.; Chang, C. C.; Schauer, J. J.; Zhang, R. Primary sources and secondary formation of organic aerosols in Beijing, China. Environ. Sci. Technol. 2012, 46 (18), 9846−9853.

(47) Du, Z.; He, K.; Cheng, Y.; Duan, F.; Ma, Y.; Liu, J.; Zhang, X.; Zheng, M.; Weber, R. A yearlong study of water-soluble organic carbon in Beijing I: Sources and its primary vs. secondary nature. Atmos. Environ. 2014, 92, 514−521.

(48) Dan, M.; Zhuang, G.; Li, X.; Tao, H.; Zhuang, Y. The characteristics of carbonaceous species and their sources in PM2.5 in Beijing. Atmos. Environ. 2004, 38 (21), 3443−3452.

(49) Duan, J.; Tan, J.; Cheng, D.; Bi, X.; Deng, W.; Sheng, G.; Fu, J.; Wong, M. Sources and characteristics of carbonaceous aerosol in two largest cities in Pearl River Delta Region, China. Atmos. Environ. 2007, 41 (14), 2895−2903.

(50) Liu, Y.; Shao, M.; Fu, L.; Lu, S.; Zeng, L.; Tang, D. Source profiles of volatile organic compounds (VOCs) measured in China: Part I. Atmos. Environ. 2008, 42 (25), 6247−6260.

(51) Pandis, S. N.; Harley, R. A.; Cass, G. R.; Seinfeld, J. H. Secondary organic aerosol formation and transport. Atmos. Environ. Part A. Gen. Top. 1992, 26 (13), 2269−2282.

(52) Liu, Y.; Shao, M.; Lu, S.; Chang, C.-C.; Wang, J.-L.; Fu, L. Source apportionment of ambient volatile organic compounds in the Pearl River Delta, China: Part II. Atmos. Environ. 2008, 42 (25), 6261−6274.

(53) Volkamer, R.; Jimenez, J. L.; San Martini, F.; Dzepina, K.; Zhang, Q.; Salcedo, D.; Molina, L. T.; Worsnop, D. R.; Molina, M. J. Secondary organic aerosol formation from anthropogenic air pollution: Rapid and higher than expected. Geophys. Res. Lett. 2006, 33 (17), L17811.

Table 1 Summarized dataset for $PM_{2.5}$ collected in winter of Guangzhou (n=48)

	Mean	Std.	Min.	Max.
$PM_{2.5}$	74.6	24.2	38.7	138
WSOC	4.08	2.01	0.89	8.11
WIOC	6.69	3.96	1.38	20.5
OC	10.8	5.31	2.41	25.5
EC	2.12	1.68	0.21	8.26
TC	12.9	6.81	2.77	33.8
WSOC/EC	2.70	1.64	0.61	8.11
WIOC/EC	4.00	2.08	2.03	12.0
OC/EC	6.70	3.23	2.94	17.9
Cl^-	1.33	1.24	0.13	6.11
Na^+	0.26	0.14	0.08	0.63
NH_4^+	5.10	2.12	1.30	9.76
NO_3^-	5.76	3.45	1.18	14.9
K^+	0.77	0.37	0.20	1.55
SO_4^{2-}	10.6	4.41	2.66	19.4
NO_3^-/SO_4^{2-}	0.57	0.25	0.09	1.02
Gal	11.1	6.45	1.79	27.8
Man	24.2	13.6	3.67	57.1
Lev	432	301	55.9	1640
Unidentified $PM_{2.5}$	37.9	10.1	17.5	70.0

Note: all fractions are in the unit of $\mu g/m^3$ except Gal, Man and Lev (ng/m^3)

Table 2 Fractions of contemporary carbon (f_c) for different types of carbon measured

	WSOC	WIOC	EC	OC	TC
GIG01	0.69±0.03	0.66±0.03	0.32±0.01	0.68±0.05	0.63±0.05
GIG02	0.65±0.03	0.55±0.03	0.09±0.01	0.57±0.04	0.45±0.04
GIG03	0.62±0.03	0.61±0.03	0.40±0.02	0.61±0.04	0.60±0.05
GIG04	0.73±0.04	0.54±0.03	0.36±0.02	0.60±0.04	0.58±0.05
GIG05	0.68±0.03	0.60±0.03	0.26±0.01	0.63±0.04	0.58±0.04
GIG06	0.66±0.03	0.64±0.03	0.30±0.01	0.65±0.04	0.61±0.05
GIG07	0.70±0.03	0.70±0.03	0.38±0.02	0.70±0.05	0.66±0.05
GIG08	0.65±0.03	0.53±0.03	0.18±0.01	0.58±0.04	0.49±0.04
Average	0.67±0.03	0.60±0.06	0.29±0.10	0.63±0.04	0.58±0.07

Table 3 Concentrations for different carbon fractions (μg/m^3)

	Based on ^{14}C						Based on SOA tracers						
	EC_{bb}	EC_f	OC_{f_pri}	OC_{bb}	OC_{f_sec}	OC_{bio_sec}	SOC_M	SOC_I	SOC_β	$SOC_{M+I+\beta}$	SOC_A	$SOC_{M+I+\beta+A}$	TC
GIG01	0.11±0.01	0.24±0.02	0.46±0.03	0.43±0.08	0.32±0.02	1.20±0.11	0.05	0.01	0.01	0.07	0.08	0.14	2.77
GIG02	0.77±0.06	7.49±0.56	9.29±0.51	7.00±1.33	1.80±0.12	7.45±1.48	0.52	0.03	0.79	1.35	0.32	1.66	33.8
GIG03	0.14±0.01	0.21±0.02	0.84±0.05	0.49±0.09	0.71±0.05	1.98±0.14	0.16	0.01	0.16	0.32	0.09	0.41	4.36
GIG04	0.24±0.02	0.43±0.03	1.73±0.09	3.01±0.57	0.51±0.04	0.42±0.59	0.05	0.01	0.01	0.06	0.02	0.09	6.33
GIG05	0.54±0.04	1.56±0.12	3.02±0.16	4.56±0.86	1.84±0.13	3.89±0.93	0.41	0.03	0.37	0.81	0.49	1.30	15.4
GIG06	0.55±0.04	1.29±0.10	2.03±0.11	5.05±0.96	2.77±0.19	3.88±1.03	0.56	0.03	0.58	1.17	0.48	1.65	15.6
GIG07	0.66±0.05	1.09±0.08	2.04±0.11	6.54±1.24	2.29±0.16	3.47±1.31	0.55	0.03	0.48	1.07	0.53	1.60	16.1
GIG08	0.92±0.07	4.18±0.31	5.41±0.29	3.78±0.72	2.54±0.17	7.12±0.85	0.66	0.03	0.48	1.17	0.60	1.77	24.0
Average	0.49±0.28	2.06±2.38	3.10±2.74	3.86±2.31	1.60±0.90	3.68±2.39	0.37±0.23	0.02±0.01	0.36±0.26	0.75±0.49	0.33±0.22	1.08±0.68	14.8±9.83

Note: OC_{f_pri} denotes primary fossil fuel organic carbon. The f_{soc} for isoprene (0.155), β-caryophyllene (0.023) and aromatic (0.00797) are obtained from previous chamber experiment.[32] Since only 3-hydroxyglutaric acid and pinonic acid that accounted for 26.5% of all monoterpene SOA tracer[32] were analyzed in here, the f_{soc} of monoterpene suggested for 0.231 in chamber experiment was transferred to 0.061 based on this proportion.

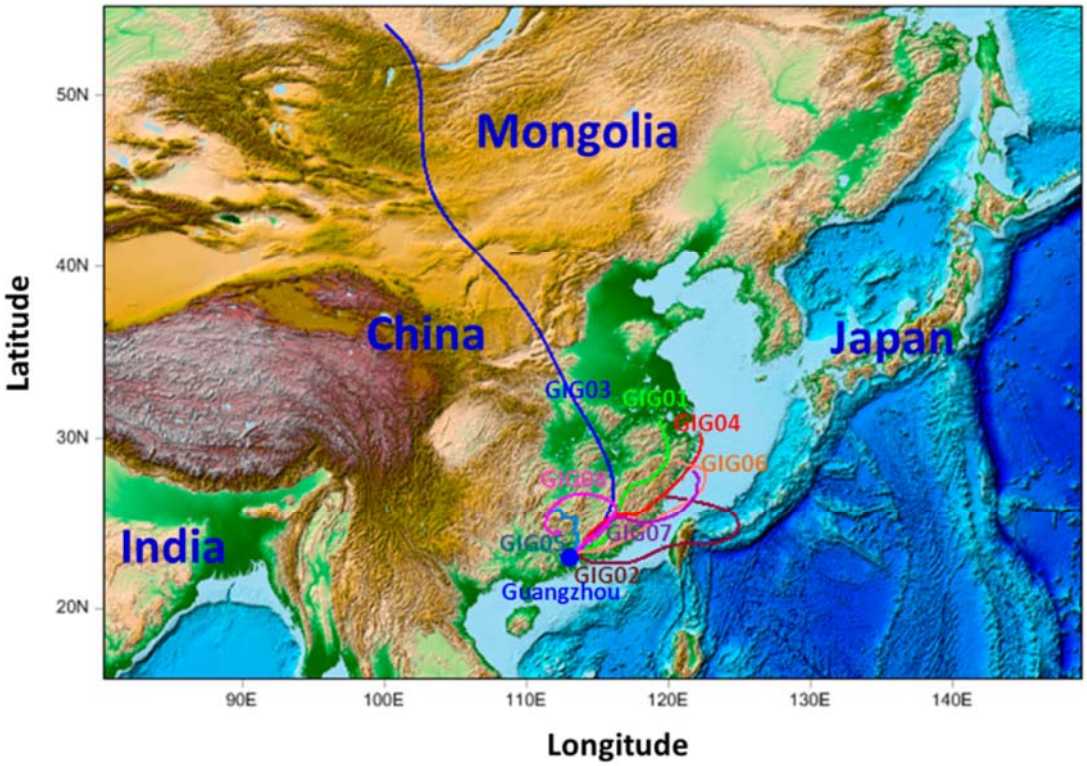

Figure 1 Sampling sites and the 72 hours air mass back trajectories for selected samples at 100 m above ground level modeled by Air Resources Laboratory, National Oceanic and Atmospheric Administration (http://ready.arl.noaa.gov/HYSPLIT.php)

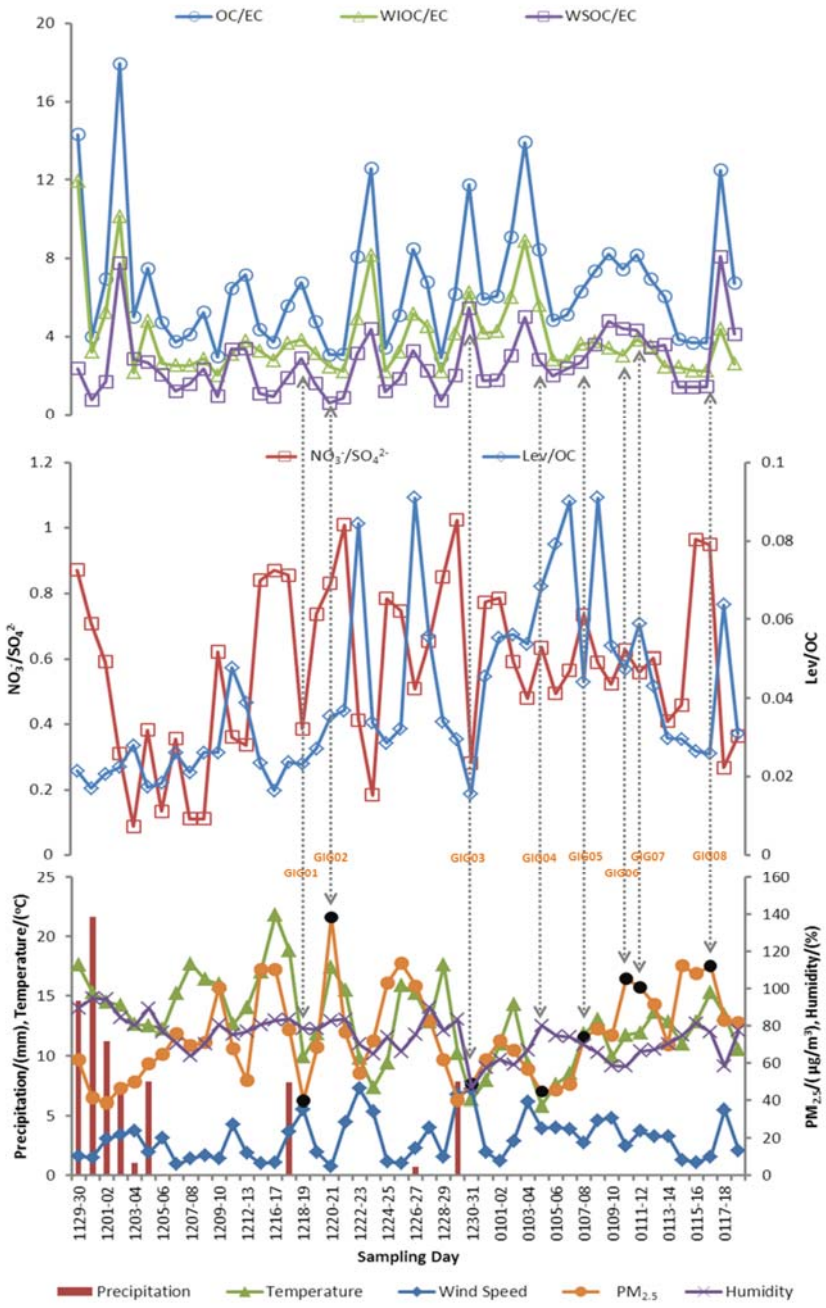

Figure 2 Time series between November 2012 and January 2013 of $PM_{2.5}$ concentrations, chemical ratios and meteorological parameters. The 8 black filled dots (GIG01-08) are the samples selected for the measurements of ^{14}C and SOA tracers. Of which, GIG02, GIG06, GIG07 and GIG08 are typical haze samples with highest $PM_{2.5}$ levels (>100 μg/m^3)

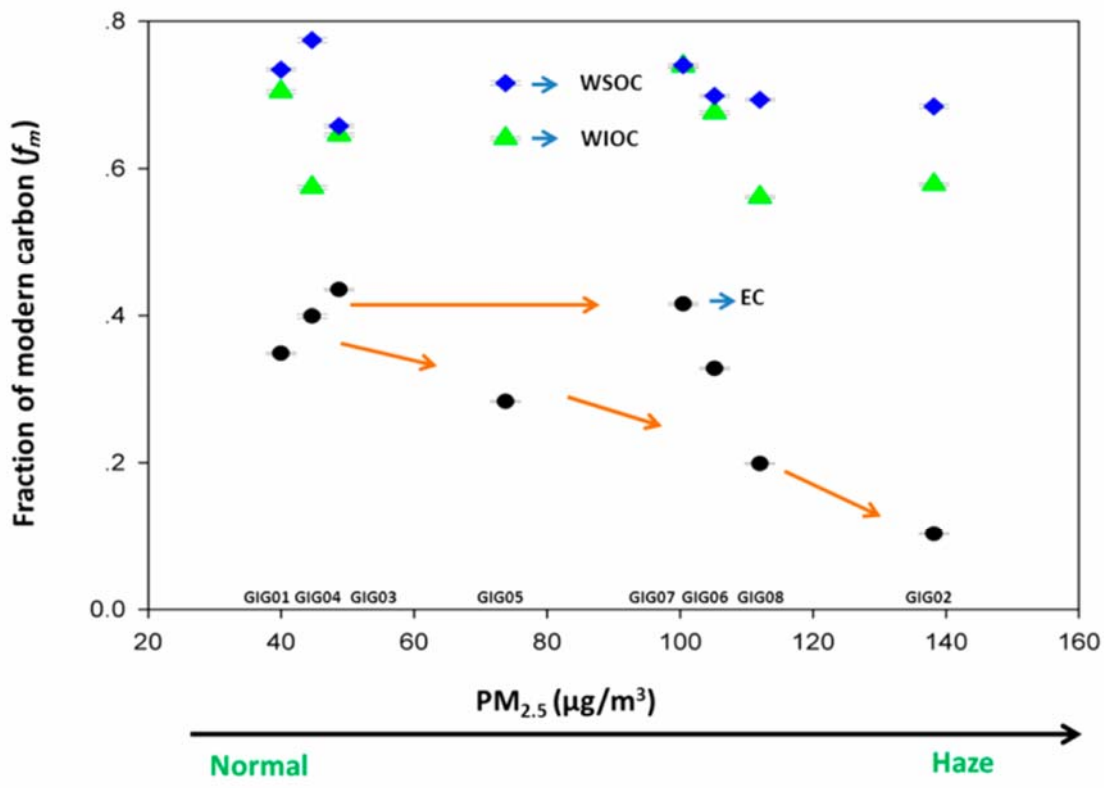

Figure 3 Fraction of modern carbon versus $PM_{2.5}$ concentration.

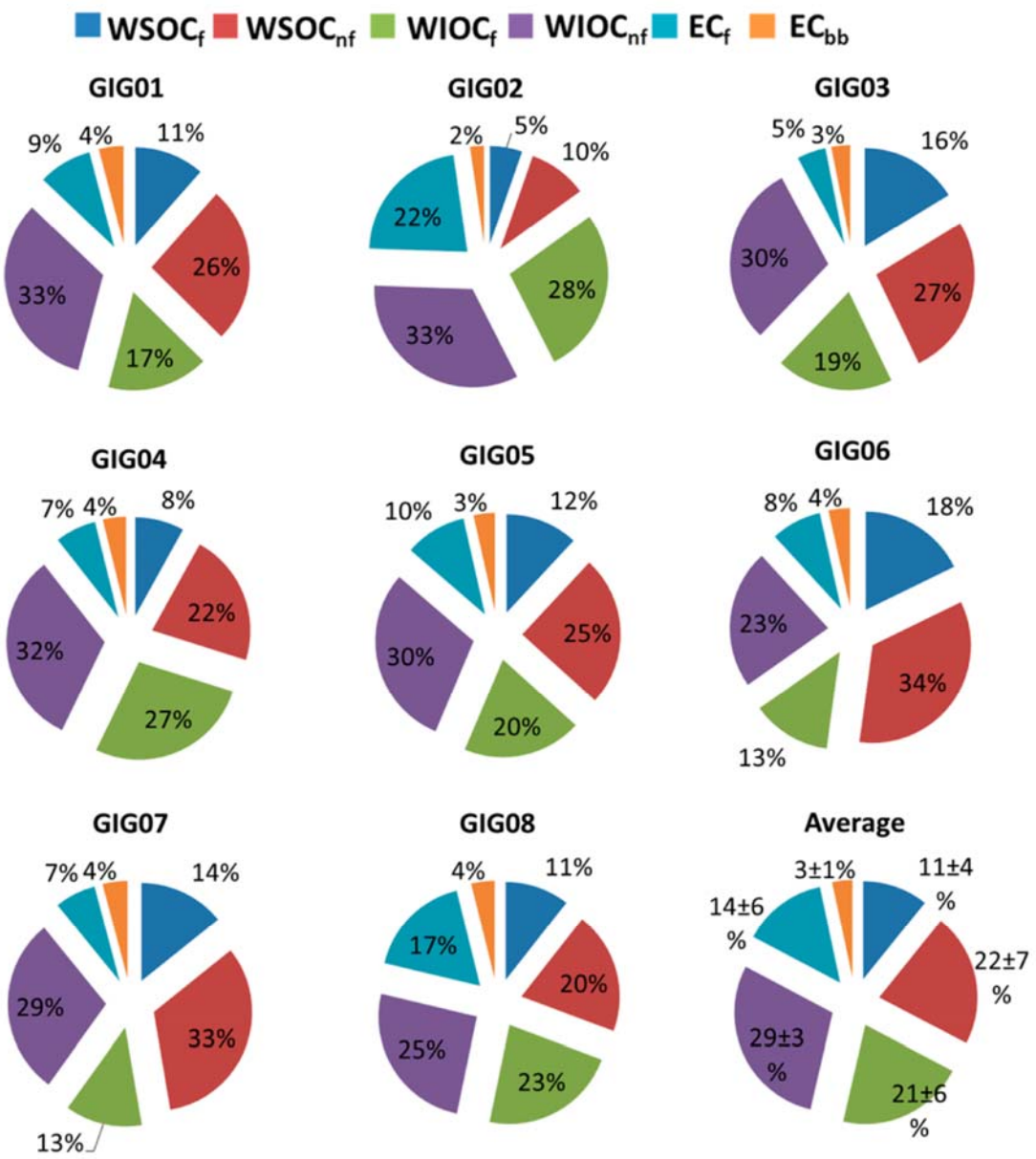

Figure 4 ^{14}C-derived source apportionment for TC

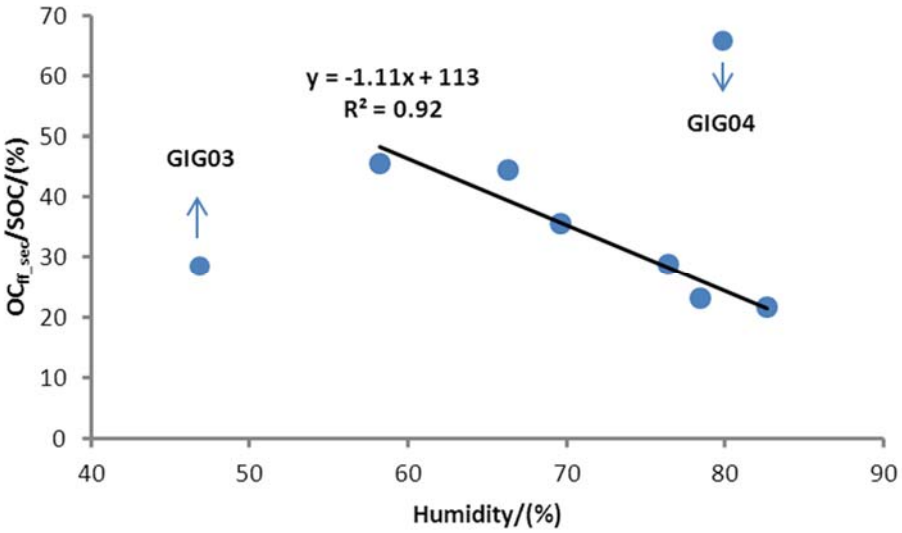

Figure 5 OC_{f_sec}/SOC versus humidity